Algorithms for Local Sensor Synchronization

Lixing Wang, Yin Yang, Xin Miao, Dimitris Papadias, Yunhao Liu

Department of Computer Science and Engineering, Hong Kong University of Science and Technology

Clear Water Bay, Hong Kong

{lxwang, yini, miao, dimitris, liu}@cse.ust.hk

Abstract— **In a wireless sensor network (WSN), each sensor monitors environmental parameters, and reports its readings to a base station, possibly through other nodes. A sensor works in *cycles*, in each of which it stays active for a fixed duration, and then sleeps until the next cycle. The frequency of such cycles determines the portion of time that a sensor is active, and is the dominant factor on its battery life. The majority of existing work assumes *globally synchronized WSN* where all sensors have the same frequency. This leads to waste of battery power for applications that entail different accuracy of measurements, or environments where sensor readings have large variability.**

To overcome this problem, we propose LS, a query processing framework for *locally synchronized* WSN. We consider that each sensor n_i has a distinct *sampling frequency* f_i, which is determined by the application or environment requirements. The complication of LS is that n_i has to wake up with a *network frequency* $F_i \geq f_i$, in order to forward messages of other sensors. Our goal is to minimize the sum of F_i without delaying packet transmissions. Specifically, given a routing tree, we first present a dynamic programming algorithm that computes the optimal network frequency of each sensor; then, we develop a heuristic for finding the best tree topology, if this is not fixed in advance.

I. INTRODUCTION

A sensor is a device with a radio and limited computation capabilities, which takes physical measurements such as temperature, light and humidity. A wireless sensor network (WSN) consists of a *base station* that collects measurements and/or aggregate information, and a set of sensor nodes, each of which is able to directly communicate with other sensors (or the base station) within the area of its radio coverage. Users register continuous queries at the base station, which are processed based on the sensor measurements. The transmission of sensor readings to the base station are performed according to the *topology* of the WSN, which can be either tree-based (e.g., [12]) or multi-path (e.g., [17]). This work follows the tree-based paradigm due to its simplicity and high energy efficiency.

In most applications, especially WSN deployed in harsh or difficult to access environments, sensor battery power is the main bottleneck of the entire system. In order to minimize energy consumption, instead of sensors being on continuously, they operate in *cycles*. Specifically, within a cycle, each sensor is active for a fixed duration, during which it (i) collects measurements from the environment, (ii) receives data from other sensors in its network neighborhood, (iii) possibly performs computations[1] on the received and collected measurements, (iv) broadcasts data to the WSN, and then enters the *sleep* mode until it *wakes* up for the next cycle.

The power consumption of a sensor is dominated by the time that its radio remains on [9][18][21]. Accordingly, since a sensor switches on its radio for a fixed duration in every cycle, its energy cost is proportional to the *frequency* of the cycles. Existing work has focused on query processing in globally synchronized WSN, where all sensors have the same frequency. This leads to waste of battery power for applications that entail different accuracy of measurements (depending on the sensor location), or environments where sensor readings have large variability. To overcome this problem, we propose LS (for *local synchronization*), a novel framework that permits sensors to have different frequencies. For instance, in a factory setting, temperature sensors in engine rooms, or other areas susceptible to fire, must sample much more frequently than sensors in warehouses. In other cases, the different frequencies may be imposed by the variability of measurements, e.g., a sensor that has stable readings for long periods should turn on less often than another whose readings change with a high rate.

Let the *sampling frequency* f_i of sensor node n_i be the minimum frequency by which n_i should turn on in order to take measurements. Given f_i, the goal of LS is to determine a *network frequency* F_i of each sensor n_i so that: (i) F_i is at least as high as f_i in order to satisfy the accuracy requirements, (ii) n_i is active when it needs to forward messages from other sensors to the base station, and (iii) the sum of network frequencies for all sensors in the WSN is minimized. Fig. 1a shows an example subtree of a WSN containing three sensors n_1-n_3 and their sampling frequencies f_1-f_3. Sensor n_1 is in the path of n_2 and n_3; i.e., it must forward messages from these sensors to the base station, implying that n_1 should be active whenever n_2 and n_3 are active. Fig. 1b and Fig. 1c illustrate two solutions towards this. In Fig. 1b, the network frequency F_2 of n_2 increases with respect to its sampling frequency ($\Delta_2=F_2-f_2=1$), achieving synchronization of n_1 and n_2 (n_1 and n_3 are already synchronized). Consequently, n_2 can sample with higher frequency (3 instead of 2) since its energy consumption is dominated by the radio. In Fig. 1c, the network frequencies F_1 and F_3 become 4, whereas $F_2=f_2=2$ (i.e., n_2 wakes up once for every two cycles of n_1 and n_3). The first solution is better because the total increase ($\Sigma\Delta_i$) of the network frequency compared to the sampling frequency is

[1] In case of *in-network* query processing, sensor nodes perform local computations instead of simply forwarding raw data; e.g., for a *max* query, a sensor computes and transmits only the maximum among the received values and the local measurement (instead of all values).

smaller (1 versus 2). Since the sampling frequencies are fixed and given, minimizing $\Sigma\Delta_i$ is equivalent to minimizing the total network frequencies.

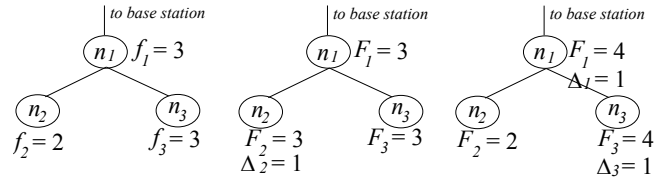

(a) Sampling frequencies (b) Optimal network frequencies (c) Suboptimal network frequencies

Fig. 1 Subtree with three sensor nodes

Searching for the optimal network frequencies in a WSN is a challenging task, for two reasons. First, there is an infinite search space for the network frequency F_i of a node n_i, which can be any real number satisfying $F_i \geq f_i$ so that n_i is synchronized with the sensors directly connected to it. Second, locally optimal solutions do not necessarily lead to globally optimal ones. Fig. 2a extends the subtree of Fig. 1a by adding two more sensors n_4 and n_5, with f_4=2 and f_5=4. Fig. 2b expands the solution of Fig. 1b to this setting. Given that F_1=3, the best values for the network frequencies of n_4 and n_5 are F_4=F_5=6 (i.e., a multiple of F_1=3), yielding $\Sigma\Delta_i$=7 ($\Delta_2+\Delta_4+\Delta_5$). On the other hand, by expanding the solution of Fig. 1c, we obtain the network frequencies of Fig. 2c, which are minimal ($\Sigma\Delta_i$=4) for this setting.

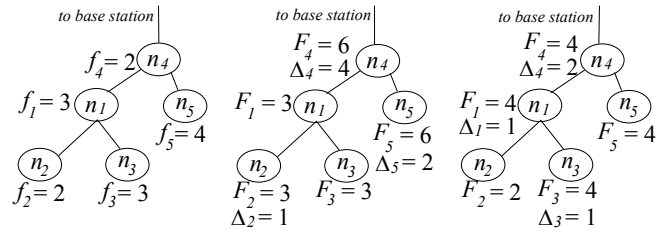

(a) Sampling frequencies (b) Suboptimal network frequencies (c) Optimal network frequencies

Fig. 2 Subtree with five sensor nodes

The problem is more complex when the tree topology is not given, but it has to be computed so that it minimizes $\Sigma\Delta_i$. To our knowledge, the only previous work [11] on locally synchronized WSN requires proxies. On the other hand, LS achieves energy-efficient local synchronization without additional hardware. Specifically, (i) given a tree topology, we compute the optimal network frequencies through a polynomial-time dynamic programming algorithm; (ii) we employ effective heuristics to obtain a high-quality tree topology, if this is not fixed in advance. Extensive experiments demonstrate that LS leads to substantial energy savings compared to the globally synchronized framework.

The rest of the paper is organized as follows. Section II surveys related work. Section III formally defines two key tasks in local synchronization: the computation of the optimal network frequencies and the tree topology. Section IV and V provides efficient algorithms for the above tasks, respectively. Section VI examines the effectiveness of the proposed algorithms using real and synthetic WSN data. Section VII concludes the paper.

II. Related Work

Section II-A overviews data transmission in WSN. Section II-B surveys WSN query processing methods that minimize energy consumption.

A. Data Transmission in a WSN

Due to their limited radio range, most sensors in the WSN cannot transmit directly to the base station, but must communicate with the latter through other sensors. These connections are represented by a connectivity graph G where: (i) every node $n_i \in G$ corresponds to a sensor (we use the terms *sensor* and *node* interchangeably), and (ii) an edge $(n_i, n_j) \in G$ denotes that sensors n_i, n_j are within the radio range of each other[2]. Fig. 3a shows a graph consisting of five sensors n_1 to n_5, and a base station n_0; n_1 and n_2 can communicate directly with the base station n_0. On the other hand, n_3, n_4 and n_5 must relay their messages through n_1 and n_2. Since there are multiple choices for n_3-n_5 to reach the base station, the WSN must select a *routing scheme* that determines the routing path for each message.

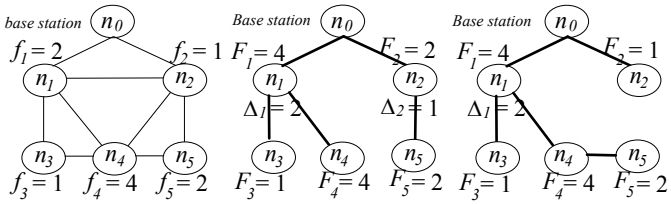

(a) Connectivity graph (b) Suboptimal tree (c) Optimal tree

Fig. 3 Tree topologies for WSN

A large class of routing schemes organizes sensors in tree topologies [13]. Specifically, a spanning tree is built from the connectivity graph, with the base station acting as the root. Most approaches only consider *min-hop* trees, in order to minimize packet losses [8]. A spanning tree $T \subseteq G$ is min-hop, if and only if the number of edges between every node n_i and n_0 is the minimum among all possible paths in G. For example, the tree in Fig. 3b is min-hop, whereas that in Fig. 3c, is not because n_5 needs 3 hops to reach n_0 and there is a shorter path n_5-n_2-n_0 in G. In multi-path routing schemes [2][17], a message may arrive at the base station through several paths. In the example of Fig. 3a, a data packet from n_4 may be transmitted to both n_1 and n_2. Compared with routing trees, multi-path schemes are more robust, at the cost of higher energy consumption and duplicate packets received by the base station. Manjhi et al. [15] propose *Tributaries-and-Deltas*, combining tree and multi-path routing.

In our work we consider tree topologies. However, in our setting, conventional minimum spanning tree algorithms (i.e., Prim's and Kruskal's) do not necessarily minimize the network frequency. Fig. 3b illustrates a counter-example using Prim's algorithm that starts with a single node and keeps adding the edge with the minimum cost, which is defined as the Δ_i incurred in the path from the new node to the sink. We begin with the base station n_0 and insert all edges that connect

[2] We assume that all edges in G are undirected, which holds in most practical WSNs [14].

it with nodes (n_1, n_2) within its range. Assuming that n_0 is always on, these edges have zero cost. Then, n_3 is appended as a child of n_1 also with zero cost. Subsequently, the algorithm adds node n_5, which increases the frequency of n_2 to 2 ($\Delta_2 = 1$), and finally n_4 with cost $\Delta_1 = 2$. The overhead of this tree measured by $\Sigma\Delta_i$ is 3. On the other hand, the optimal spanning tree in Fig. 3c has cost 2. The complication is due to the fact that edge weights are not constant, but keep changing according to the nodes already inserted in the tree.

B. Query Processing in WSN

WSN query processing techniques can be classified into three categories, depending on their restrictions on the sensors' sampling and network frequencies. Methods (e.g., [3], [19], [20], [22]) in the first category assume that all sensors have the same sampling frequency f. The second class consists of techniques (e.g., [12], [13]) that allow different sensors to have different sampling rates, but require that they use the same network frequency $F=\max\{f_i \mid \forall n_i\}$. Finally, the methods of [11] provide flexibility on frequency assignment using additional base-station-like devices called *proxies* that form the backbone of the WSN. Specifically, (i) each sensor is assigned to one proxy; (ii) all the sensors assigned to the same proxy have the same frequency; and (iii) sensors assigned to different proxies may have different frequencies. The use of proxies, however, limits the applicability of [11], since they increase the financial costs of the WSN system, as well as the difficulty for its deployment.

Besides the above, the network community has proposed Low Power Listening (LPL) [7], a low-level protocol for *unsynchronized* WSNs that allows sensors to have arbitrary working cycles. Unlike synchronized WSNs, in LPL a sensor n_i may be asleep when another node n_j needs it to forward a message. When this happens, n_j postpones the message, and keeps probing n_i by continuously sending *preamble signals*, until n_i wakes up and responds. The two sensors then perform the delayed data transmissions. Due to such delays, LPL may not be suitable for applications with strict responsiveness requirements. Furthermore, the sender of the preamble signals (i.e., n_j) must stay active for long periods, which drains up its battery power. The above problems amplify as the height of the routing tree increases. In contrast, the proposed methods do not incur any result delays or prolonged transmissions of control signals.

III. Problem Definition

Let f_i be the *sampling frequency* of sensor node n_i; f_i is a real number determined by the application requirements on accuracy, or the variability of measurements. The proposed LS (*local synchronization*) assigns to each n_i an individual network frequency F_i, rather than a global one. In practice, since the work cycle of a sensor must be sufficiently long to complete the necessary sensing, computation and communication tasks, its network frequency must not exceed a constant F_{max}. Let N be the total number of sensors excluding the base station. Our goal is to minimize the objective function $\Phi=\sum_{i=1}^{N} F_i$, referred to as the *cost* of the WSN. This cost determines the total time that sensors are active, and therefore, it dominates the overall energy consumption. The proposed methods can be easily extended to other aggregates such as maximum and weighted sum. We assume that the WSN uses a tree topology T, which guides the routing of messages between sensors. Table I summarizes frequent symbols.

TABLE I
SUMMARY OF NOTATIONS

Symbol	Meaning
G, T	WSN connectivity graph and routing tree
N	Number of sensors in the WSN
Φ	Cost of the WSN
n_i	i-th sensor (if $1\le i\le N$), or the base station (if $i=0$)
f_i, F_i	Sampling and network frequency of n_i
F_i^{LB}	Lower bound of F_i defined in Lemma 2
F_{max}	Maximum possible network frequency
T_i	Subtree of T rooted at n_i
$\Phi_i^{F_i}$	Minimum cost of subtree T_i for a given F_i

Each sensor must be able to communicate with the base station, in order to report its measurements and / or in-network computation results. To model this, we first introduce the concept of local synchronization between two directly connected sensors.

Definition 1 (Local Synchronization): Given a routing tree T, an internal node n_i, and its child n_j, n_i and n_j are locally synchronized (or simply *synchronized* when the context is clear), if and only if (i) n_i and n_j start one of their respective cycles at the same time, and (ii) there exists a positive integer k such that $F_i=k\cdot F_j$.

Intuitively, when a node n_i is synchronized with its child n_j, n_i is able to process and / or forward every message from n_j on time. Among the two conditions in the Definition 1, (i) is a low-level networking issue, e.g., the clocks of the two sensors need to be synchronized[3], whereas (ii) restricts the sensors' network frequencies in LS query processing. Hence, in the following we assume that (i) is always satisfied. We next model our main constraint.

Lemma 1: Every sensor is able to communicate with the base station n_0 in each cycle, if and only if every pair of parent-child nodes in T are locally synchronized.

Based on whether T is given, we distinguish two different versions of the problem. The first, referred to as Problem 1, takes T as an input (e.g., determined by an existing algorithm based on link quality considerations [6]), and computes the network frequencies of the sensors that minimize Φ. In the second version (Problem 2), T is unknown; instead, given the WSN connectivity graph G, LS selects both the optimal topology $T\subseteq G$ and the network frequencies to minimize Φ. Compared with Problem 1, the additional flexibility on T may

[3] Small differences between n_i's and n_j's clocks are tolerable, as long as the two sensors can finish message transmissions in one common working cycle. Furthermore, LS requires only local clock synchronization (e.g., [4], [5]), which is less demanding than global clock synchronization of all sensors in the WSN (e.g., [10]).

lead to further reduction of Φ, at the expense of an enlarged search space. Formally, we state the above two problems as follows.

Problem 1: Given a routing tree T and the sampling frequency f_i of each node n_i, compute the network frequency F_i of each n_i so that (i) $F_{max} \geq F_i \geq f_i$, (ii) every pair of parent-child sensors in T are locally synchronized and (iii) $\Phi=\sum_{i=1}^{N} F_i$ is minimized.

Problem 2: Given the connectivity graph G and the sampling frequency f_i of each node n_i, find the best routing tree $T \subseteq G$ that minimizes $\Phi=\sum_{i=1}^{N} F_i$, where the network frequency F_i of each sensor n_i is computed according to Problem 1.

Unfortunately, we have the following negative result.

Theorem 1: Problem 2 is NP-hard.

Proof: (by reduction to set cover) Given an instance of the set cover problem that involves a set E of elements and another S of subsets, construct a corresponding connectivity graph G as follows. G contains the base station n_0, as well as two layers of sensors. For each subset $s \in S$ (resp. element $e \in E$) in the set cover instance, we create a first-layer (resp. second-layer) node in G. Furthermore, whenever a subset s contains an element e in the set cover instance, we add an edge connecting n_s and n_e in G, where n_s and n_e are the corresponding nodes of s and e, respectively. Additionally, there is an edge in G between each node on the first layer and the base station n_0. The sampling frequency of every first-layer (resp. second-layer) node is 1 (resp. 2). Then, we solve Problem 2 with the above G to obtain the optimal routing tree T. The set of first-layer nodes in T that are parent to at least one second-layer node correspond to the optimal solution of the set cover instance. Therefore, Problem 2 is at least as hard as set cover. Moreover, first-layer (resp. second-layer) nodes always require 1 (resp. 2) hops to the reach the base station in any spanning tree of G. Therefore, the routing tree $T \subseteq G$ is always min-hop, meaning that Problem 2 is still as hard as set cover under the min-hop limitation. □

In the following, we describe solutions to both problems. In addition, we discuss their extensions to the case when the routing tree (in Problem 1) or the connectivity graph (in Problem 2) changes over time.

IV. Finding Network Frequencies

This section focuses on Problem 1, i.e., optimal network frequency computation with a given routing tree T. Section IV-A lays down the theoretical foundation of the proposed solution. Section IV-B describes an efficient dynamic programming algorithm, and analyses its space and time complexity. Section IV-C provides further optimizations.

A. Theoretical Foundation

We first investigate the range of feasible values for the network frequency F_i of a node n_i. Apart from f_i, there is a tighter lower bound for F_i, as follows.

Lemma 2: Given a node n_i and the subtree $T_i \subseteq T$ rooted at n_i, a lower bound for the network frequency F_i of n_i is

$$F_i^{LB} = \max\{f_j \mid \forall n_j \in T_i\} \quad (1)$$

Proof: (by induction) For any node $n_j \in T_i$, clearly $F_j \geq f_j$ according to the problem definition. Suppose that a node n_x is along the path from n_j to n_i whose network frequency F_x satisfies that $F_x \geq f_j$. Let n_y be the parent node of n_x. Since n_x and n_y are locally synchronized, we have $F_y \geq F_x \geq f_j$. By induction, $F_i \geq f_j$. □

For instance, in Fig. 2a, the network frequency F_4 of n_4 must be no smaller than $F_i^{LB}=\max\{f_1, f_2, f_3, f_4, f_5\}=4$. Observe that $f_4=2<F_i^{LB}$; consequently, f_4 in our example *does not have any impact on the choice of* F_4. To avoid complicated notations, in the rest of Section IV-A we assume that for each sensor n_i, $f_i=F_i^{LB}$; whenever this is not the case, F_i^{LB} is used in place of f_i.

However, besides F_{max}, there is no obvious upper bound for F_i. Fig. 4a shows an example subtree rooted at sensor n_1, which has two children n_2 and n_3. The sampling frequencies are $f_1=13$, $f_2=5$, and $f_3=11$, respectively. Suppose that n_2 (resp. n_3) have Cl_2 (resp. Cl_3) child nodes, which all have identical sampling frequencies to their respective parent. The marginal cost of increasing F_2 (resp. F_3) is then multiplied by Cl_2+1 (resp. Cl_3+1), as every child of n_2/n_3 must also increase their network frequency by the same amount to synchronize with their respective parent. Fig. 4b lists several values for F_1 and the corresponding F_2 and F_3 that minimizes the overall cost of T_1, while satisfying the synchronization requirements. The best F_1 depends on Cl_2 and Cl_3: when both n_2 and n_3 have numerous (e.g., >50) children, the best F_1 is 55, which in our example is a common multiple of both f_2 and f_3, and thus, minimizes the cost of the subtrees T_2 and T_3. Observe that this is far larger than either one of f_1-f_3. In general, f_2 and f_3 can be non-integer values (e.g., 3.1 and 9.7), in which case the best F_1 may exceed even the product of f_2 and f_3, depending on the number of children attached to n_2 and n_3.

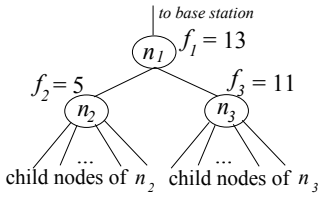

(a) Subtree T_1

F_1	F_2	F_3
13	6.5	13
14	7	14
15	5	15
16	16/3	16
20	5	20
21	5.25	21
22	5.5	11
55	5	11

(b) Network frequencies

Fig. 4 Example of choosing network frequencies

The above example also demonstrates that there is an infinite search space for a network frequency value (F_1), rendering even a brute-force solution rather complicated. We tackle the problem using a *top-down* approach. Two key issues are (i) how to determine the network frequencies of top-level nodes that are directly connected to the base station, and (ii) given the network frequency F_i of an internal node n_i, how to choose the network frequencies of its children. We first focus on (ii). In particular, consider a child n_j of n_i; in order to synchronize n_i and n_j, their network frequencies must satisfy that $F_i=k \cdot F_j$ for a positive integer k, according to Definition 1.

Meanwhile, since $F_j \geq f_j$, we have $k \leq \lfloor F_i/f_j \rfloor$. Hence, there is a finite number of possible F_j's.

Lemma 3: Let n_i be an internal node of T, and n_j be a child of n_i. Given the network frequency F_i of n_i, the network frequency F_j must take one of the following values

$$F_j \in \left\{ F_i/k \,\middle|\, k = 1,2,3,\ldots,\left\lfloor F_i/f_j \right\rfloor \right\} \quad (2)$$

For example, in Fig. 4, when F_1 is set to 13, according to Lemma 3, there are two possible values (13 and 13/2=6.5) for F_2, and only one (13) for F_3. The question now is how to select the best F_j for the child n_j among the above possibilities. Intuitively, since F_i is already given, the choice of F_j only affects the descendents of n_j. Accordingly, the best F_j is the one that minimizes the subtree T_j rooted at n_j.

Lemma 4: Given a node n_i, suppose that its network frequency F_i is already determined. Let $\Phi_i^{F_i}$ be the minimum cost of subtree $T_i \subseteq T$ rooted n_i with respect to F_i. Then, $\Phi_i^{F_i}$ can be computed recursively as follows:

$$\Phi_i^{F_i} = F_i + \sum_{\text{child } n_j \text{ of } n_i} \min\left\{ \Phi_j^{F_i/k} \,\middle|\, k = 1,2,\ldots \left\lfloor F_i/f_j \right\rfloor \right\} \quad (3)$$

where $\Phi_j^{F_i/k}$ is the minimum cost of subtree T_j given $F_j = F_i/k$.

Proof: Consider an arbitrary child node n_j of n_i. According to the definition of Problem 1, besides f_j, the value of F_j only affects the network frequencies of n_j's parent (i.e., F_i of n_i) and children (and, recursively, the descendents of n_j). Since F_i is fixed and given, the choice of F_j has impact only on the cost of the subtree T_j. Therefore, the best F_j should minimize the cost of T_j, which, combined with Lemma 2, leads to Equation (3). □

As a special case, when n_i is a leaf node, $\Phi_i^{F_i}$ is simply F_i. Based on Lemma 4, once F_i is determined, it is straightforward to compute $\Phi_i^{F_i}$, as well as the best network frequencies of all nodes in the subtree T_i, through exhaustive search. For instance, in Fig. 2, given F_4=6, F_5 must be 6, since f_5=4>6/2. F_1 can be either 3 or 6. In the former case, F_2=F_3=3, hence Φ_1^3 =3+3+3=9. In case that F_1=6, F_2 can be 2, 3, or 6, F_3 can be 3 or 6, and the minimum possible cost for T_1 is Φ_1^6 =6+2+3=11. Since $\Phi_1^3 < \Phi_1^6$, the best value for F_1 is 3, and, thus, Φ_4^6 =6+Φ_1^3 +6=21.

However, the number of possible values for a network frequency increases exponentially with the depth of the node in the tree topology. To reduce the number of potential values, we now describe our most important theoretical result, which entails the recursive equation (3), only if F_i is a *regular network frequency*, defined as follows.

Definition 2 (Regular Network Frequency): A network frequency F_i is regular, if and only if either (i) $F_i = f_i$ or (ii) there exists a node $n_j \neq n_i$ in the subtree T_i rooted at n_i such that $F_i = k \cdot f_j$ for a positive integer k.

For instance, among the values of F_1 listed in Fig. 4b, only 13, 15, 20, 22 and 55 are regular ones (shown in grey). In general, n_1's regular network frequencies are f_1=13 and multiples of f_2=5 (e.g., 15, 20, 55), or f_3=11 (22, 55), since all children of n_2 and n_3 have the same sampling frequencies as their respective parent.

Theorem 2: Given an internal node n_i and a network frequency F_i, let F'_i be the highest regular network frequency for n_i satisfying $F'_i \leq F_i$. Then:

$$\Phi_i^{F_i} = \Phi_i^{F'_i} \cdot F_i / F'_i \quad (4)$$

Furthermore, suppose that when F'_i is assigned to n_i, the best network frequency for each node $n_j \in T_i$ is F'_j. Then, when F_i is assigned to n_i, the optimal network frequencies for the nodes in T_i are:

$$F_j = F'_j \cdot F_i / F'_i, \forall n_j \in T_i \quad (5)$$

Proof: We first prove that Equation (5) gives a feasible solution for T_i that leads to a subtree cost of $\Phi_i^{F_i}$ given in Equation (4). Because when F'_i is assigned to n_i, F'_j is the optimal network frequency of any node n_j in T_i, it must also be a feasible network frequency for n_i. Hence, $F_j \geq F'_j \geq f_j$. Meanwhile, consider any internal node $n_x \in T_i$ and one of its children $n_y \in T_i$. Let F'_x and F'_y be the optimal network frequencies of n_x and n_y, respectively, when F'_i is assigned to n_i. Clearly, F'_x is a multiple of F'_y. Let integer $k_{xy} = F'_x / F'_y$. According to Equation (5), $F_x / F_y = F'_x / F'_y = k_{xy}$. Hence, F_x is a multiple of F_y, which enables the local synchronization of n_x and n_y. Additionally, we have

$$\Phi_i^{F_i} = \sum_{n_j \in T_i} F_j = \sum_{n_j \in T_i} \frac{F'_j \cdot F_i}{F'_i} = \frac{F_i}{F'_i} \cdot \sum_{n_j \in T_i} F'_j = \frac{\Phi_i^{F'_i} \cdot F_i}{F'_i} \quad (6)$$

Next we prove by induction that $\Phi_i^{F_i}$ given in Equation (4) is indeed the minimum cost when F_i is assigned to n_i. In the base case, n_i is a leaf node in T. The theorem holds trivially, since $\Phi_i^{F_i} = F_i$, and $\Phi_i^{F'_i} = F'_i$. In the induction step, suppose that each child node n_j of n_i satisfies the theorem. Specifically, given an arbitrary node n_x, let the function $CR_x(F_x)$ that returns the highest regular network frequency for n_x satisfying that $CR_x(F_x) \leq F_x$. As a special case, $CR_i(F_i) = F'_i$. The induction assumption is stated as follows.

$$\forall \text{child } n_j \text{ of } n_i, \forall F_j, \frac{\Phi_j^{F_j}}{F_j} = \frac{\Phi_j^{CR_j(F_j)}}{CR\left(F_j\right)} \quad (7)$$

According to Lemma 2, when F_i is assigned to n_i, F_j must be F_i/k for a positive integer $k \leq \lfloor F_i/f_j \rfloor$. Similarly, when F'_i is assigned to n_i, F_j must be F'_i/k for a positive integer $k \leq \lfloor F'_i/f_j \rfloor$. We now prove that $\lfloor F_i/f_j \rfloor = \lfloor F'_i/f_j \rfloor$ by contradiction. Suppose that $\lfloor F_i/f_j \rfloor \neq \lfloor F'_i/f_j \rfloor$. Then, since $F'_i \leq F_i$, we have $\lfloor F'_i/f_j \rfloor < \lfloor F_i/f_j \rfloor$, and, thus, $F'_i < \lfloor F_i/f_j \rfloor \cdot f_j \leq F_i$. However, $\lfloor F_i/f_j \rfloor \cdot f_j$ a regular frequency for n_i, as it is an integer multiple of f_j. This contradicts with the fact that F'_i is the largest regular network frequency for n_i satisfying $F'_i \leq F_i$.

Substituting F_j with F_i/k and F'_i/k in Equation (7), respectively, we obtain

$$\forall k = 1,2,\cdots \left\lfloor F_i/f_j \right\rfloor, \frac{\Phi_j^{F_i/k}}{F_i/k} = \frac{\Phi_j^{CR_j(F_i/k)}}{CR_j\left(F_i/k\right)} \quad (8)$$

$$\forall k = 1,2,\cdots \left\lfloor F_i / f_j \right\rfloor, \frac{\Phi_j^{F_i'/k}}{F_i'/k} = \frac{\Phi_j^{CR_j(F_i'/k)}}{CR_j\left(F'/k\right)} \tag{9}$$

Next we prove $CR_j(F_i/k)=CR_j(F'_i/k)$ by contradiction. Suppose that $CR_j(F_i/k)\neq CR_j(F'_i/k)$. Because $F'_i<F_i$, $CR_j(F'_i/k)<CR_j(F_i/k)$. Hence, $F'_i<CR_j(F_i/k)\cdot k\leq F_i$. Since $CR_j(F_i/k)$ is a multiple of f_x of a node n_x in $T_j\subseteq T_i$, and k is a positive integer, $CR_j(F_i/k)\cdot k$ is also a multiple of f_x, meaning that $CR_j(F_i/k)\cdot k$ is a regular network frequency for n_i that is closer to F_i than F'_i, which contradicts with the definition of F'_i. Therefore, $CR_j(F_i/k)=CR_j(F'_i/k)$, and, consequently, the right hand side of Equation (8) equals that of Equation (9). Their respective left hand side must be equal as well:

$$\frac{\Phi_j^{F_i/k}}{F_i} = \frac{\Phi_j^{F_i'/k}}{F_i'} \tag{10}$$

Let $k^*\leq\lfloor F_i/f_j\rfloor$ be the positive integer satisfying:

$$\forall k = 1,2,\cdots \left\lfloor F_i / f_j \right\rfloor, \Phi_j^{F_i'/k^*} \leq \Phi_j^{F_i'/k} \tag{11}$$

According to Lemma 3 and the fact that $\lfloor F_i/f_j\rfloor=\lfloor F'_i/f_j\rfloor$, we have

$$\Phi_i^{F_i'} = F_i' + \sum\nolimits_{\text{child } n_j} \Phi_j^{F_i'/k^*} \tag{12}$$

Multiplying both sides of Inequality (11) by F_i/F'_i, we obtain

$$\forall k = 1,2,\cdots \left\lfloor F_i / f_j \right\rfloor, \frac{\Phi_j^{F_i'/k^*} \cdot F_i}{F_i'} \leq \frac{\Phi_j^{F_i'/k} \cdot F_i}{F_i'} \tag{13}$$

Combining Equation (10) and Inequality (13), we obtain

$$\forall k = 1,2,\cdots \left\lfloor F_i / f_j \right\rfloor, \Phi_j^{F_i/k^*} \leq \Phi_j^{F_i/k} \tag{14}$$

Therefore, according to Lemma 3, we have

$$\begin{aligned} \Phi_i^{F_i} &= F_i + \sum\nolimits_{\text{child } n_j} \Phi_j^{F_i/k^*} \\ &= F_i + \sum\nolimits_{\text{child } n_j} \frac{\Phi_j^{F_i'/k^*} \cdot F_i}{F_i'} \\ &= \frac{F_i}{F_i'}\left(F_i' + \sum\nolimits_{\text{child } n_j} \Phi_j^{F_i'/k^*}\right) \\ &= \frac{\Phi_i^{F'} \cdot F_i}{F'} \end{aligned} \tag{15}$$

The second line in the above equation is based on Equation (10), whereas the last step is based on Equation (12). Therefore, the theorem also holds for n_i. □

In the example of Fig. 4, consider an irregular frequency F_1=16. F'_1=15 is the highest regular frequency satisfying $F'_1\leq F_1$. According to Fig. 4b, when F_1=16 is assigned to n_1, the optimal values for F_2 and F_3 are 16/3 and 16 respectively. Meanwhile, when F'_1= 15 is assigned to n_1, the best network frequencies for n_2 and n_3 are F'_2=5 and F'_3=15 respectively. Clearly, $\Phi_1^{16}/\Phi_1^{15}=F_2/F'_2=F_3/F'_3=16/15$.

Theorem 2 indicates that $\Phi_i^{F_i}$ is a piece-wise linear function of F_i. Specifically, as F_i grows from one regular value to the next one, $\Phi_i^{F_i}$ increases linearly with F_i; when F_i reaches the next regular value, $\Phi_i^{F_i}$ suddenly drops. Subsequently, $\Phi_i^{F_i}$ again increases linearly with F_i until the next regular frequency, possibly with a different slope. Fig. 5 plots $\Phi_1^{F_1}$ against F_1 in the example of Fig. 4, assuming that n_2 and n_3 have 2 and 3 child nodes respectively. Regular frequencies for n_1 between 13 and 55 are shown on the x-axis. The piece-wise linear pattern, as well as the sudden drops in $\Phi_1^{F_1}$ at regular values for F_1, can be clearly observed in the plot.

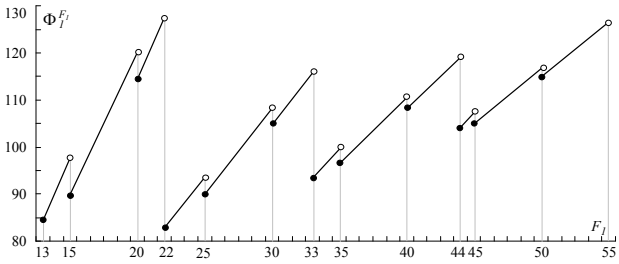

Fig. 5 Example plot of $\Phi_i^{F_i}$ vs. F_i

Another consequence of Theorem 2 is that an irregular F_i always leads to a higher subtree cost than the corresponding regular value F'_i preceding F_i. Therefore, for each top-level node n_i for which there is no restriction on its network frequency F_i, it suffices to consider only its regular values of F_i.

Corollary 1: Given a node n_i that is directly connected to the base station, the optimal network frequency of n_i must be regular.

For a node n_j whose parent is another sensor n_i, its network frequency is restricted to the values described in Lemma 3. Consequently, given a irregular frequency F_j of n_j, the highest regular frequency F'_j preceding F_j may not be able to synchronize with n_i. Hence, the best frequency for F_j can be irregular. For such nodes, the following algorithm utilizes Theorem 2 to reduce the computation of $\Phi_j^{F_j}$ to that of $\Phi_j^{F'_j}$.

B. Algorithm

Given the routing tree T and the sampling frequencies $f_1, f_2, \ldots, f_N$, LS searches for the optimal network frequencies F_1^*-F_N^* in two steps. First, it computes the minimum cost Φ^* of the entire WSN and gradually completes a hash table H. Second, guided by H, LS finds the optimal values F_1^*-F_N^* that sum up to Φ^*. The hash table H contains entries of the form $\langle n_i,F_i\rangle\rightarrow\Phi_i^{F_i}$, where the key is a node n_i and a regular frequency F_i for n_i, and the value $\Phi_i^{F_i}$ is the minimum cost of the subtree T_i rooted at n_i, given F_i.

The first step involves two functions, namely *CTC* (short for *compute total cost*) and CSC (for *compute subtree cost*). Fig. 6 illustrates *CTC*. The method initially computes the lower bound F_i^{LB} for the network frequency F_i of each node n_i (lines 2-4). According to Lemma 2, F_i^{LB} is a tighter bound than f_i; whenever $f_i<F_i^{LB}$, the latter is used instead (specifically, in Equations (2), (3), and Definition 2). After that, the algorithm examines each top-level node n_i, and computes the minimum cost Φ_i^{min} of the subtree T_i rooted at n_i (lines 5-10). In particular, line 7 enumerates all regular values for F_i that may possibly lead to the Φ_i^{min}, according to Corollary 1. Line 8

invokes the recursive procedure *CSC* (described below) to compute $\Phi_i^{F_i}$; the smallest $\Phi_i^{F_i}$ among all values of F_i becomes Φ_i^{min}. Finally, line 10 sums up Φ_i^{min} for all top-level nodes to obtain the minimum overall cost Φ^*.

CTC(T, f_1-f_N): returns Φ^* //CTC for compute total cost
// Input: T: routing tree, f_1-f_N: sampling frequencies of the sensors
// Output: Φ^*: optimal cost of the entire WSN
1. Initialize Φ^* to 0, and H to an empty hash table
2. For each node $n_i \in T$
3. Compute F_i^{LB} according to Equation (1)
4. If $F_i^{LB} > f_i$, use F_i^{LB} in place of f_i in the rest of the algorithm
5. For each n_i that is directly connected to the base station in T
6. Initialize Φ_i^{min} to $+\infty$
7. For each regular F_i
8. Call $\Phi_i^{F_i} = CSC(T, f_1$-$f_N, n_i, F_i, H)$
9. If $\Phi_i^{F_i} < \Phi_i^{min}$, set Φ_i^{min} to $\Phi_i^{F_i}$
10. Update Φ^* to $\Phi^* + \Phi_i^{min}$
11. Return Φ^*

Fig. 6 Algorithm *CTC*

Fig. 7 shows *CSC*, which recursively computes the optimal cost $\Phi_i^{F_i}$ of the subtree T_i rooted at node n_i, given F_i. When F_i is irregular, the algorithm picks the highest regular frequency F'_i satisfying $F'_i \le F_i$, calculates $\Phi_i^{F'_i}$, and applies Theorem 2 to obtain $\Phi_i^{F_i}$ (lines 1-4). On the other hand, when F_i is regular, Lemma 4 is used to compute $\Phi_i^{F_i}$ recursively (lines 6-13). The result is stored in a new entry of the hash table H with key $<n_i, F_i>$. When the same parameters n_i, F_i are passed to *CSC*, the latter looks up H for the stored $\Phi_i^{F_i}$ (line 5).

CSC (T, f_1-f_N, n_i, F_i, H): returns $\Phi_i^{F_i}$ // CSC for compute subtree cost
// Input: T: routing tree
// f_1-f_N: sampling frequencies of the sensors
// n_i, F_i: root node of the subtree T_i, and its network frequency
// H: hash table storing subtree costs
// Output: $\Phi_i^{F_i}$: minimum subtree cost of T_i given F_i
1. If F_i is irregular with respect to n_i
2. Let $F'_i < F_i$ be the highest regular network frequency for n_i
3. Call $\Phi_i^{F'_i} = CSC(T, f_1$-$f_N, n_i, F'_i, H)$
4. Calculate $\Phi_i^{F_i}$ according to Equation (4), and return $\Phi_i^{F_i}$
5. If H contains an entry with key $<n_i, F_i>$ and value $\Phi_i^{F_i}$, return $\Phi_i^{F_i}$
6. If n_i is a leaf node, return F_i
7. Initialize $\Phi_i^{F_i}$ to F_i
8. For each child n_j of n_i
9. Initialize Φ_j^{min} to $+\infty$
10. For each value of F_j described in Equation (2)
11. Call $\Phi_j^{F_j} = CSC(T, f_1$-$f_N, n_j, F_j, H)$
12. If $\Phi_j^{F_j} < \Phi_j^{min}$, set Φ_j^{min} to $\Phi_j^{F_j}$
13. Update $\Phi_i^{F_i}$ to $\Phi_i^{F_i} + \Phi_j^{min}$
14. Add a new entry to H with key $<n_i, F_i>$ and value $\Phi_i^{F_i}$
15. Return $\Phi_i^{F_i}$

Fig. 7 Algorithm *CSC*

Fig. 8 describes the function *CNF* (short for *compute network frequencies*), which implements the second step of the proposed solution, and computes the optimal frequencies top-down. The method starts by examining each top-level node n_i, testing regular network frequencies F_i of n_i (lines 3-7). Since F_i is regular, and *CTC* has called *CSC* with parameters n_i and F_i, the hash table H already contains an entry $<n_i, F_i> \rightarrow \Phi_i^{F_i}$. The value of F_i that minimizes the subtree cost for T_i becomes the optimal frequency F_i^* of n_i. After determining the optimal frequencies for all top-level nodes, the algorithm continues to calculate the frequencies of their descendents. Specifically, given a node n_i with known F_i^* and one of its children n_j, *CNF* enumerates all possible values for F_j, and computes the minimum cost for subtree T_i. For a regular F_j, $\Phi_j^{F_j}$ is simply retrieved from H. When F_j is irregular, $\Phi_j^{F_j}$ is obtained using Theorem 2 and H. In both cases, there is no need for recursive calls, since the computations have already been performed in *CSC*, and the results stored in H.

CNF (T, f_1-f_N): returns F_1^*-F_N^*
// CNF for compute network frequencies
// Input: T: routing tree, f_1-f_N: sampling frequencies of the sensors
// Output: F_1^*-F_N^*: optimal network frequencies of the nodes in T
1. Call $\Phi^* = CTC(T, f_1$-$f_N)$
2. Let H be the hash table used in *CTC*
3. For each node n_i that is directly connected to the base station n_0
4. Initialize Φ_i^{min} to $+\infty$, F_i^* to NULL
5. For each regular F_i
6. Retrieve $\Phi_i^{F_i}$ from H with key $<n_i, F_i>$
7. If $\Phi_i^{F_i} < \Phi_i^{min}$, set Φ_i^{min} to $\Phi_i^{F_i}$, and F_i^* to F_i
8. Repeat
9. For each node n_j satisfying (i) F_j^* has not been determined and (ii) F_i^* corresponding to the parent n_i of n_j has been determined
10. Initialize Φ_j^{min} to $+\infty$, F_j^* to NULL
11. For each value of F_j described in Equation (2)
12. Compute $\Phi_j^{F_j}$ using H and Theorem 2
13. If $\Phi_j^{F_j} < \Phi_j^{min}$, set Φ_j^{min} to $\Phi_j^{F_j}$, and F_j^* to F_j
14. Until all optimal network frequencies are determined
15. Return F_1^*-F_N^*

Fig. 8 Algorithm *CNF*

Fig. 9 illustrates an example of the above algorithms. Assume that F_{max}=100 according to the application requirements. The sampling frequencies are shown alongside their corresponding nodes. Among them, f_3 is smaller than the lower bound F_3^{LB} given by Lemma 2, which equals the maximum sampling frequency (i.e., f_6=11) in the subtree rooted at n_3. Therefore, in the computation of the optimal network frequencies, the algorithms simply discard the original value f_3=2, and proceed as if f_3 were F_3^{LB}=11.

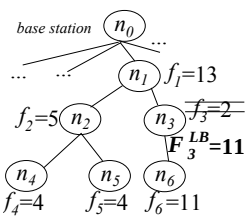

(a) Sampling frequencies

n_i	F_i	$\Phi_i^{F_i}$
n_2	5	15
n_2	12	20
n_3	11	22
n_1	13	58.5
n_1	15	60
…		

(b) Hash table H

1	*CSC*(n_1,13)
2	*CSC*(n_2, 6.5)
3	*CSC*(n_2, 5)
4	*CSC*(n_4, 5)
5	*CSC*(n_5, 5)
6	*CSC*(n_2, 13)
7	*CSC*(n_2, 12)
…	

(c) Calls of CSC

Fig. 9 Example of network frequency computation

Next we elaborate the computation of the optimal F_1^*- F_5^* in the subtree T_1 rooted at n_1. Since n_1 connects directly to n_0, *CTC* enumerates all its regular frequencies, which include (i) f_1=13 and (ii) all multiples of f_2=5, f_4=f_5=4, and F_3^{LB}=f_6=11 below F_{max}=100. Assume that *CTC* first assigns F_1=13, and invokes *CSC* to compute Φ_1^{13}. Fig. 9c shows the 7 subsequent calls to *CSC*, listing only parameters n_i and F_i since the others remain the same for all invocations of *CSC*. In the first call *CSC*(n_1, 13), the hash table H does not have an entry with key <n_1, 13>; thus, *CSC* computes Φ_1^{13} recursively by identifying the best value for the network frequencies F_2 and F_3 of n_1's child nodes n_2 and n_3, given that F_1=13. We first focus on F_2. According to Lemma 3, there are two possible values for F_2: F_1=13 and F_1/2=6.5. Suppose that *CSC* first calculates $\Phi_2^{6.5}$ by recursively calling *CSC*(n_2, F_2=6.5). However, 6.5 is not a regular frequency for n_2 because it is not equal to f_2=5, or a multiple of f_4=f_5=4. Therefore, CSC finds the highest regular frequency F'_2=5 below 6.5, and calls CSC(n_2, 5).

To compute Φ_2^5, which has no corresponding entry in H, *CSC* must determine the best F_4 and F_5 given F_2=5. According to Lemma 3, there is only one possible value 5 for both F_4 and F_5. In the next two steps, *CSC* calls itself with parameters (n_4, 5) and (n_5, 5) respectively, which return Φ_4^5 =Φ_5^5=5. With this information, the third call to CSC (i.e., with parameters n_2 and 5) returns Φ_2^5=5+Φ_4^5+Φ_5^5 =15, after adding a new entry <n_2, 5>=15 to H. Subsequently, the second call to *CSC* with parameters n_2 and 6.5 then returns $\Phi_2^{6.5}$ =Φ_2^5 ·6.5/5=19.5, according to Theorem 2. Next, the first call *CSC*(n_1, 13) tests the other possible F_2=13 for n_2 by calling *CSC*(n_2, 13), which leads to another invocation *CSC*(n_2, 12) with the highest regular network frequency 12 below 13. The latter eventually returns Φ_2^{12}=20, and after *CSC*(n_2, 13) we have Φ_2^{13}=Φ_2^{12}·13/12=65/3. Because $\Phi_2^{6.5}$<Φ_2^{13}, the minimum cost for subtree T_2 given F_1=13 is $\Phi_2^{6.5}$=19.5. The first call *CSC*(n_1, 13) then computes the minimum cost for subtree T_3 rooted at n_3, which is 26 when F_3=F_6=13. Accordingly, Φ_1^{13}= 13+19.5+26 = 58.5, concluding the computation of *CSC*(n_1, 13).

The outer function *CTC* then computes minimum subtree costs of T_1 with other regular values of F_1, e.g., 15, 16, 20, 22, etc. Finally, *CTC* establishes that Φ_1^{13} =58.5 is the minimum cost for subtree T_1 among all values of F_1. After the termination of *CTC*, *CNF* computes the optimal network frequencies top-down. *CNF* enumerates all regular values of F_1 and finds the one with the minimum $\Phi_1^{F_1}$ using the hash table H. Having determined that F_1^*=13, *CNF* continues to calculate F_2^*, F_3^*, and subsequently F_4^*-F_6^* based on the optimal subtrees stored in H.

Theorem 3: The space and time complexity of the algorithmic framework is $O(N^2 \cdot C)$ and $O(N^2 \cdot C^2)$, respectively, where $C=\lfloor F_{max}/f_{min} \rfloor$, and $f_{min}=\min\{f_i | 1 \le i \le N\}$.

Proof: We first prove that algorithm *CTC* takes $O(N^2 \cdot C)$ space and $O(N^2 \cdot C)$ time. Its space consumption is dominated by the storage of the hash table H, which consists of entries of the form $<n_i,F_i> \rightarrow \Phi_i^{F_i}$, where n_i is an arbitrary node, F_i is a regular network frequency for n_i, and $\Phi_i^{F_i}$ is the minimum cost of the subtree T_i rooted at n_i, when F_i is assigned to n_i. According to Definition 2, F_i must be a multiple of the sampling frequency f_j of a node $n_j \in T_i$. Since $F_i \le F_{max}$ and $f_j \ge f_{min}$, the number of possible regular network frequencies for n_i contributed by n_j is upper bounded by $C=\lfloor F_{max}/f_{min} \rfloor$. Since n_j can be any of the $O(N)$ nodes in T_i, the total number of regular network frequencies for n_i is $O(N \cdot C)$. Considering that n_i can be any node in the WSN, the number of entries in H is $O(N^2 \cdot C)$.

Regarding time complexity, the dominating factor is the time consumed by subroutine *CSC*, which computes the optimal subtree cost for a given node n_i and its network frequency F_i. The cases when F_i is irregular, or when H contains an entry with key <n_i,F_i> take negligible time to handle. Hence, it suffices to count the invocations of *CSC* with a regular F_i and a combination of <n_i,F_i> not processed before. In each such invocation, *CSC* recursively calls itself to compute the minimum subtree cost corresponding to each child node n_j of n_i. Specifically, the algorithm considers all possible network frequencies for n_j given F_i, which is bounded by C. Let Cl_i be the number of the children of n_i, *CSC* finishes in $O(Cl_i \cdot C)$ time. Counting all calls to *CSC* with fresh and regular inputs, the total time complexity is $\sum_{n_i}$ =$O(C \cdot Cl_i \cdot N \cdot C)$=$O(N^2 \cdot C^2)$.

Next we focus on *CNF*. Clearly, its space complexity is also dominated by the storage of H, which is bounded by $O(N^2 \cdot C)$ as in *CTC*. Concerning time, after calling *CTC*, *CNF* enumerates all possible network frequencies of every node exactly once, which takes $O(N^2 \cdot C)$ time. Hence, its time complexity is also $O(N^2 \cdot C^2)$. □

C. Discussion

The value of C in Theorem 3 grows with F_{max}. Next we present optimizations to limit the impact of F_{max}, and significantly speed up network frequency computation. In the example of Fig. 9, one feasible solution is to set the network frequency of each sensor in n_1-n_6 to the highest sampling frequency f_1=13 among the 6 sensors, leading to a total cost of 78 for subtree T_1. Clearly, setting F_1>78 will always result in a higher subtree cost for T_1. Furthermore, since each sensor n_i must have a network frequency $F_i \ge F_i^{LB}$ according to Lemma 2, when F_1>43, even when n_2-n_5 use their respective minimum possible network frequency, the total cost for T_1 still exceeds that achieved with the above simple solution (i.e., 78). Therefore, it suffices to examine only regular frequencies for F_1 not exceeding 43. Note that this is a much tighter bound than F_{max}=100. In addition, after obtaining Φ_1^{13} =58.5, the upper bound for F_1 can be further tightened to 23.5, since any higher value, plus the minimum possible network frequencies of n_2-n_5, would result in a subtree cost for T_1 higher than the current best 58.5.

Based on the above observations, we modify algorithm *CTC* as follows. In line 7 of Fig. 6, the regular frequencies are enumerated in increasing order. Let $|T_i|$ be the number of

nodes in T_i; an upper bound F_i^{UB} for F_i is initialized to $\max\{f_j | n_j \in T_i\} \cdot |T_i| - \sum_{j \notin i, n_j \in T_i} F_j^{LB}$, and incrementally maintained as $\Phi_i^{min} - \sum_{j \notin i, n_j \in T_i} F_j^{LB}$ while the minimum subtree cost Φ_i^{min} for T_i gets updated. The loop of lines 7-10 terminates as soon as F_i exceeds F_i^{UB}. Let F_{UB} be the maximum value of F_i^{UB} for all nodes after CTC finishes. If $F_{max} > F_{UB}$, the latter replaces the former in the complexity analysis, since it is the actual upper bound of all network frequencies used in our algorithms.

A similar optimization applies to algorithm CSC, when computing the minimum subtree cost Φ_j^{min} (lines 10-12 in Fig. 7). Specifically, an upper bound $\Phi_j^{min} - \sum_{l \notin j, n_l \in T_j} F_l^{LB}$ for F_j is incrementally maintained, and the loop stops when F_j exceeds it. In our running example, the 6th call of CSC is eliminated, since F_2=13 plus f_4 and f_5 already exceeds the previously computed subtree cost $\Phi_2^{6.5}$=19.5, when F_2 is set to 6.5.

Finally, we discuss the adaptation of the above algorithms to changes of the routing tree T. A straightforward solution is to re-compute the network frequencies of all sensors whenever T is modified. The main challenge is to ensure that after the transition to the new network frequencies, all sensors remain locally synchronized, while satisfying their respective sampling frequency requirements. Specifically, immediately after the new tree is applied, all sensors in the WSN wake up simultaneously, start a new cycle, and switch to their new network frequencies thereafter. This method assigns the optimal network frequency to each sensor at all times, but incurs considerable cost during transitions. An alternative approach reduces the cost of transitions as follows. First, based on historical data, we partition the sensors into *dynamic nodes*, which change their respective parents frequently, and *static* ones with stable parent nodes. Then, for each minimal subtree T_i containing at least one dynamic node, we apply global synchronization to its corresponding subtree T_i, i.e., all nodes in T_i share the same network frequency. T_i is then treated as a single node in algorithms CTC, CSC and CNF, with a weight proportional to the number of nodes in T_i. Accordingly, network frequencies need to be re-computed only when at least one static node changes its parent in T, which happens infrequently.

V. Finding Routing Trees

This section focuses on Problem 2, i.e., finding the best routing tree from a given connectivity graph. Following the common practice in the WSN literature, we restrict the search space for routing schemes to *min-hop routing trees* [1]. Unfortunately, even under this additional restriction, Problem 2 is still intractable. Therefore, we resort to heuristic methods.

Based on the min-hop property, LS partitions nodes into *layers*, so that the l-th layer contains nodes requiring at least l hops to reach n_0. Clearly, in a min-hop tree, the parent of a layer-l node must reside at layer l–1. LS starts from the layer l_{max} of nodes that need the most hops to reach n_0 (i.e., the leaves of the routing tree T) and builds T bottom-up. Specifically, whenever LS examines a node n_j at level l, the subtree T_j rooted at n_j containing nodes from levels l+1 to l_{max}, has already been constructed. LS then extends T_j by adding an appropriate parent n_i of n_j. Let P_j denote the set of *candidate parents* of n_j, which consists of layer l–1 nodes that are connected to n_j in G. The selection of n_i is performed according to the following heuristics.

Heuristic 1: Given a node n_j, the parent $n_i \in P_j$ of n_j should satisfy that $f_i \geq F_j^{LB}$ (Equation 1). If no such node exists in P_j, the parent of n_j is the node n_i with the highest f_i among all nodes in P_j.

Heuristic 2: Given a node n_j, if multiple nodes in P_j have sampling frequencies no less than F_j^{LB}, the parent of n_j is the node $n_i \in P_j$, that satisfies $f_i \geq F_j^{LB}$ and minimizes $f_i / \lfloor f_i / F_j^{LB} \rfloor$.

Intuitively, Heuristic 1 aims at minimizing the value $\Delta_i = F_i - f_i$ for the parent node n_i. In particular, in order to synchronize n_i and n_j, F_i must be no less than F_j, which, in turn, is lower bounded by F_j^{LB} according to Lemma 2. Hence, the heuristic tries to pick a node $n_i \in P_j$ satisfying $f_i \geq F_j^{LB}$, in which case it is possible that Δ_i=0. When there is no such node in P_j, Δ_i is lower bounded by $F_j^{LB} - f_i$. Thus, the node n_i with the highest f_i (i.e., minimal $F_j^{LB} - f_i$) is chosen as n_j's parent. Heuristic 2, on the other hand, tries to minimize the network frequency F_j for the child node n_j. Specifically, since F_i must be a multiple of F_j, the lowest F_j is obtained, when $F_i = f_i$, and $F_j = F_i / \lfloor f_i / F_j^{LB} \rfloor = f_i / \lfloor f_i / F_j^{LB} \rfloor$ Thus, Heuristic 2 chooses the parent n_i that minimizes this value. Fig. 10 shows an algorithm that applies the above heuristics. *Find_Routing_Tree* first partitions all nodes into layers (line 1), and builds T bottom-up. If a node n_i is directly connected to the base station n_0 in G, n_0 becomes the parent of n_i. Otherwise, the best parent P_i of n_i is chosen according to Heuristic 1 (line 11) or 2 (line 12).

```
Find_Routing_Tree(G, f1-fN): returns T
// Input:  G: connectivity graph, f1-fN: sampling frequencies
// Output: T: routing tree of the WSN
1.  Partition sensor nodes into layers
2.  Let layer l_max be the deepest layer
3.  Initialize T with nodes n1-nN, and no edges
4.  For l = l_max DownTo 1
5.      For each node n_j on layer l
6.          If l=1, add edge <n0, nj> to T
7.          Else
8.              Compute F_j^LB according to Equation (1)
9.              Let P_j be the set of candidate parents of n_j
10.             If there does not exist n_i∈P_j such that f_i≥F_j^LB
11.                 Choose n_i∈P_j according to Heuristic 1
12.             Else, choose n_i∈P_j according to Heuristic 2
13.         Add edge <n_i, n_j> to T
14. Return T
```

Fig. 10 Algorithm *Find_Routing_Tree*

The algorithm takes $O(N^2)$ time (for choosing the best parent for each node) and $O(N^2)$ space (for storing G), where N is the number of sensors. Since the network frequency assignment module has the same space and time complexities with respect to N according to Theorem 3, the proposed solution to Problem 2 takes $O(N^2)$ time and space overall, meaning that it easily scales to large WSNs. Furthermore, our experiments, shown next, demonstrate that *Find_Routing_Tree* usually

identifies high-quality trees that lead to significant energy savings.

Finally, changes in the connectivity graphs are handled as follows. Whenever at least one link in the current routing tree T is broken, we re-compute T using *Find_Routing_Tree*, as well as the network frequencies of the sensors. Otherwise, *Find_Routing_Tree* is invoked periodically, and the transition process starts when a better routing tree is detected.

VI. Experimental Evaluation

We have implemented the proposed methods in C++, and carried out all experiments on a Core 2 Duo 2.6GHz PC with 2GBytes of memory. We use two real datasets, *Greenorbs* (94 sensors), *Intel Lab* (52 sensors), and a synthetic one.

***GreenOrbs* :** *GreenOrbs* [16] is deployed by our group in a forest area in China. It contains 94 active sensors measuring temperature, humidity and light per minute. In our experiments, we use the temperature readings. The WSN follows the collection tree protocol (CTP) [6]. Specifically, sensors are organized into a routing tree, which is periodically adjusted based on the current link quality conditions. We observed that during a period of 12 hours, there is only a small number of timestamps when the tree changed. Furthermore, a large part of the tree, which forms the backbone of the network remained stable throughout the testing period. Fig. 11a shows the geographic locations of the sensors and the base station, as well as the connectivity graph of the entire WSN.

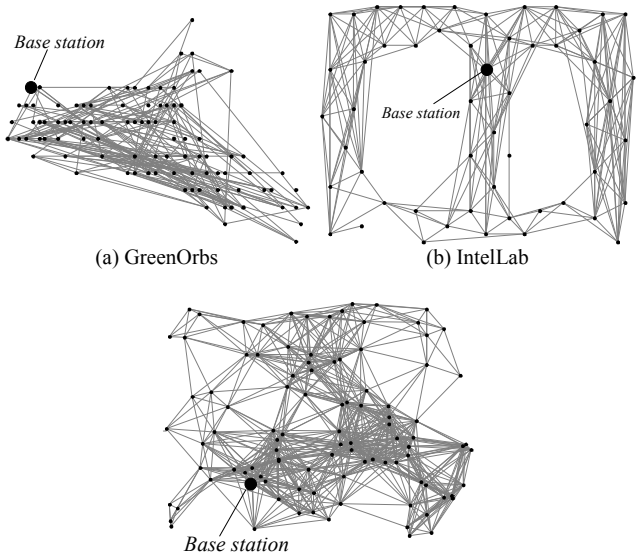

(a) GreenOrbs (b) IntelLab

(c) Synthetic (N=100)

Fig. 11 Connectivity graphs of the datasets used in the experiments

We set the sampling frequency of each sensor n_i based on the change rate of n_i's readings. The intuition is that a sensor with stable readings should sample less frequently than another whose readings change with a high rate. Specifically, suppose that node n_i has collected m samples $s_{i,1}$, $s_{i,2}$, …, $s_{i,m}$ at m timestamps $t_{i,1}$, $t_{i,2}$, …, $t_{i,m}$. The change rate cr_i of n_i is calculated by:

$$cr_i = \frac{\sum_{j=1}^{m-1} \left| s_{i,j+1} - s_{i,j} \right|}{\sum_{j=1}^{m-1} t_{i,j+1} - t_{i,j}} \quad (16)$$

Let f_{max} be the highest sampling frequency required by the application. The sampling frequency f_i of a node n_i is then:

$$f_i = \frac{cr_i \cdot f_{max}}{\max_{j=1}^{N} cr_j} \quad (17)$$

In our experiments, we use f_{max}=20. Note that the specific value of f_{max} does not affect the relative performance of the proposed methods. The maximum possible sampling frequency F_{max} is set to $10 \cdot f_{max}$=200. In all experimental settings, during the search for the optimal network frequencies, the algorithms always terminate earlier (i.e., using the optimizations described in Section IV-C) without testing the last regular frequency before F_{max}.

***IntelLab*:** *IntelLab* [4] includes data from 54 sensors that measure temperature, humidity, light and voltage every 31 seconds for a month. Similarly to *GreenOrbs*, we use temperature readings in the experiments. The sampling frequencies of the sensors are computed using Equations (16) and (17). The dataset does not include the connectivity graph G; instead, it lists the probability for each sensor n_i to successfully deliver a message directly to a surrounding node n_j. Accordingly, we add an edge $\langle n_i, n_j \rangle$ to G, whenever the probability of successful packet delivery between n_i and n_j is above 20%. Except for one sensor (ID=5), all others are connected in G. Meanwhile, the dataset does not mention the location or the connectivity of the base station. Hence, we simply treat sensor with ID 1 as the base station. Fig. 11b shows the resulting connectivity graph. Finally, there is no information on the routing tree.

Synthetic: We generate sensor locations uniformly within a [0,1]×[0,1] square. In the connectivity graph G, there is an edge $\langle n_i, n_j \rangle$, if and only if, the distance between nodes n_i and n_j does not exceed 0.25. Fig. 11c displays the connectivity graph of 100 sensors. Additionally, the sampling frequencies are random numbers in the range [1, 100], which follow the Zipf distribution. Similar to the real datasets, the maximum possible network frequency F_{max} is set to $10 \cdot f_{max}$=1000.

We investigate the energy savings and computational cost of LS, under four parameters: (i) number of nodes, (ii) distribution of the sampling frequencies, (iii) shape of the routing tree, and (iv) the number of dynamic nodes (i.e., with frequently changing parents). Sections VI-A and VI-B present results on real and synthetic datasets, respectively.

A. Results for GreenOrbs and IntelLab

GreenOrbs and *IntelLab*, like most WSN currently under deployment, are restricted to relatively few nodes (under 100), for which the computational overhead of LS is negligible. Therefore, we defer the discussion on this cost for the

[4] Available at *http://db.csail.mit.edu/labdata/labdata.html*

synthetic data, and focus on the energy overhead. Specifically, let t_w be the number of time units that a sensor is active per cycle, and P be the energy consumed per time unit. Given the sum of network frequencies Φ, the energy consumed by all sensors is $\Phi \cdot P \cdot t_w$, which is proportional to Φ. Hence, in the following we simply report the value of Φ as the overall energy cost. We compare LS against the traditional globally synchronized (GS) approach, which sets the network frequency of each sensor to $f_{max}=\max\{f_1,f_2,\ldots,f_N\}$. Clearly, the energy cost of GS is $\Phi=N \cdot f_{max}$. We include two versions of LS: *LS-Problem1* and *LS-Problem2*. The former considers a given routing tree T, whereas the latter computes T.

We first evaluate the impact of the number of nodes N on the total energy cost Φ, with a static tree T. Specifically, for *GreenOrbs*, LS-Problem1 uses a real routing tree T_{real}, taken at an arbitrary timestamp. To vary N, we randomly remove leaf nodes from T_{real} (and recursively, entire subtrees). *IntelLab*, on the other hand, does not include real routing trees. Hence, we evaluate only LS-Problem2, and vary N by removing random nodes. The sampling frequency of each node n_i is fixed to the value computed based on the real change rate of n_i's readings, as described in the beginning of this section. Fig. 12 plots Φ as a function of N. Clearly, Φ grows with N for both LS and GS, since more sensors naturally lead to higher energy consumption. Comparing GS with LS, the former consumes significantly more energy, and the difference increases with N (note the logarithmic scale on the vertical axis). This is because when a new node n_i is added, GS always assigns $F_i = f_{max}$; LS, on the other hand, usually sets F_i to be far lower than f_{max} since n_i only needs to locally synchronize with its adjacent nodes. LS-Problem2 outperforms LS-Problem1, indicating that the proposed solution indeed generates better routing trees.

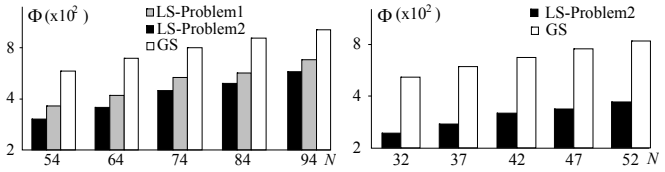

(a) GreenOrbs (b) IntelLab

Fig. 12 Energy cost Φ vs. number of nodes N

Next, we fix N to its maximum value, and study the effect of the sampling frequencies in the range [1, 100], generated according to Zipf distribution with skewness factor α. LS-Problem1 (resp. LS-Problem2) uses the real routing tree (resp. tree computed by the proposed heuristics) as before. Fig. 13 demonstrates the effect of α on Φ. Given the small node cardinality, a growing value of a decreases the probability that f_{max} reaches its maximum value 100. Consequently, the cost of all methods drops. LS takes better advantage of this fact since it can isolate the effect of the high frequencies in their respective subtrees.

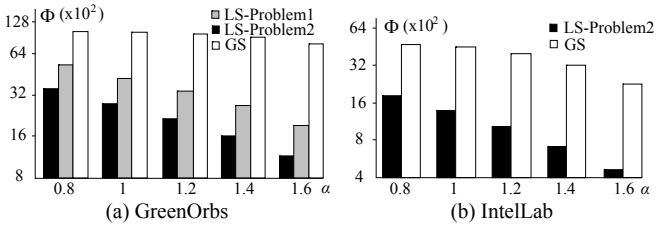

(a) GreenOrbs (b) IntelLab

Fig. 13 Energy cost Φ vs. sampling frequency skewness α

Finally, we evaluate the impact of changing routing trees. Our implementation of LS is based on the second method discussed at the end of Section IV, which minimizes re-computations of network frequencies. In the *GreenOrbs* dataset, we identified 41 dynamic nodes among the real routing trees, which reside at the lowest levels of the tree. On average, network frequency re-computations are performed once every 40 times when T changes, which itself happens infrequently. Overall, LS using real routing trees achieves 34% energy savings compared to GS. To further investigate the effect of routing trees with different volatility, we randomly mark a number N_D of nodes as dynamic in a bottom-up fashion, and evaluate the energy efficiency of LS. The total number of nodes N is fixed to its maximum value, and the sampling rates are derived from real readings. Fig. 14 demonstrates Φ against varying N_D. The energy consumption of LS generally increases with N_D, as more nodes are merged and share the same network frequencies. When the majority of sensors are dynamic, LS reduces to GS. Nevertheless, LS achieves considerable energy savings, even for relatively large values of N_D (~50% of N).

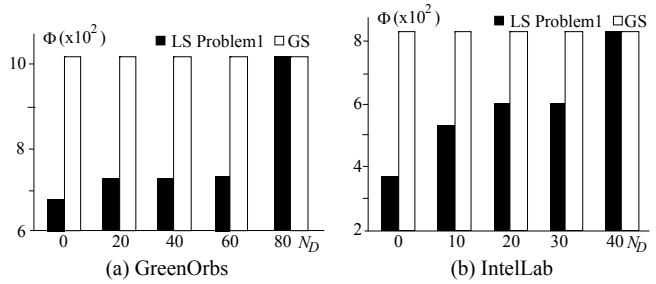

(a) GreenOrbs (b) IntelLab

Fig. 14 Energy cost Φ vs. number of dynamic nodes N_D

B. Results for Synthetic Datasets

We repeat our experiments on a much larger synthetic dataset described in the beginning of this section. In addition to energy cost, we report the CPU time and the memory required by the proposed algorithms. We focus on static routing trees; the results for changing trees lead to similar conclusions as in *GreenOrbs* and *IntelLab*, and are omitted. Fig. 15 shows the effect of the number of nodes N, after fixing the skewness factor α of the sampling frequencies to 0.8. Similar to the real datasets, the energy overhead of all methods increases with N, and LS consistently outperforms GS. The CPU and memory overhead of LS grows quadratically with N, as predicted by Theorem 3. Nevertheless, even for N=10000, these costs are very low (i.e., less than 320 milliseconds and 7Mbytes), which confirms that the proposed algorithms could be utilized for WSN much larger than the ones currently deployed.

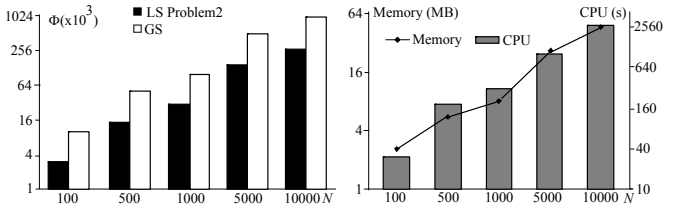

(a) Energy cost (b) Computational cost

Fig. 15 Varying number of nodes

Fig. 16 fixes N=5000, and varies the skewness factor α of the sampling frequencies. Observe that, unlike the case of real datasets, the energy consumption of GS remains the same for all values of α because, due to the large number of nodes, there is always one that has the maximum sampling frequency 100. On the other hand, as α grows, the consumption of LS decreases for the reasons explained in the context of Fig. 13. The computational overhead of LS also drops because a lower Φ leads to a more restrictive upper bound on a node's network frequency. Consequently, the optimization of Section IV-C becomes more effective, leading to an earlier termination of the algorithm.

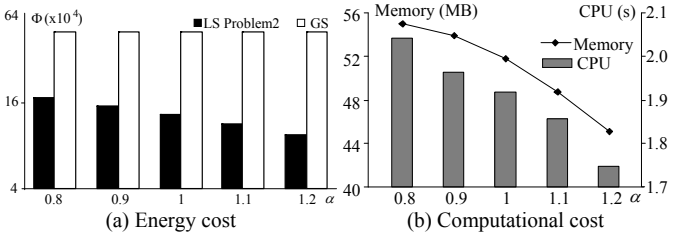

(a) Energy cost (b) Computational cost

Fig. 16 Varying the distribution of sampling frequencies

Fig. 17 investigates the impact of the routing tree on LS-Problem1. Specifically, we generate random trees with a given fanout *fan* for each internal node, and present the average of their results, after setting N=5000 and α=0.8. Since *fan* has no effect on GS, we report the ratio between the energy cost of LS and that of GS. The energy savings of LS increase with *fan* due to the fact that the height of the tree decreases; thus, a node n_i with high f_i influences fewer ancestors. The computational overhead also increases with *fan* because a higher fanout leads to a larger subtree for each internal node, and, consequently, more regular network frequencies to examine.

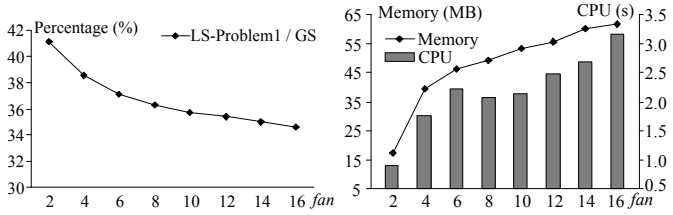

(a) Energy cost (b) Computation cost

Fig. 17 Varying the shape of the tree

VII. Conclusion

This paper presents a novel framework that allows sensors to sample at different rates, while ensuring timely routing of packets. We focus on two versions of the problem, depending on whether the WSN topology is fixed or not. Extensive experiments, using real and synthetic datasets, demonstrate the effectiveness of local synchronization in both versions. In the future we plan to investigate the computation of routing trees that minimize the network frequencies and at the same time minimize the packet losses. Finally, another interesting direction is the extension of the proposed techniques to multi-path topologies.

References

[1] Akyildiz, I., Su, W., Sankarasubramaniam, Y., Cayirci, E. Wireless Sensor Networks: a Survey. *Computer Networks*, 38(4):393-422, 2002.

[2] Considine, J., Li, F., Kollios, G., Byers, J. Approximate Aggregation Techniques for Sensor Databases. *ICDE*, 2004.

[3] Deshpande, A., Guestrin, C., Madden, S., Hellerstein, J. M., Hong, W. Model-Driven Data Acquisition in Sensor Networks. *VLDB*, 2004.

[4] Elson, J., Roemer, K. Wireless Sensor Networks: A New Regime for Time Synchronization. *Computer Communication Review*, 33(1):149-154, 2003.

[5] Ganeriwal, S., Kumar, R., Srivastava, M. Timing-Sync Protocol for Sensor Networks. *ACM SenSys*, 2003.

[6] Gnawali, O., Fonseca, R., Jamieson, K., Moss, D., Levis, P. Collection Tree Protocol. *ACM SenSys*, 2009.

[7] Jurdak, R., Baldi, P., Lopes, C. Adaptive Low Power Listening for Wireless Sensor Networks. *IEEE TMC*, 6(8):988-1004, 2007.

[8] Kim, S., Fonseca, R. Reliable Transfer on Wireless Sensor Networks. *IEEE SECON*, 2004.

[9] Levis, P., Gay, D. *TinyOS Programming*. Cambridge University Press, 2009.

[10] Li, Q., Rus, D., Global Synchronization in Sensor Networks. *IEEE Transactions on Computers*, 55(2):214-226, 2006.

[11] Madden, S., Franklin, J. Fjording the Stream: An Architecture for Queries over Streaming Sensor Data. *ICDE*, 2002.

[12] Madden, S., Franklin, M., Hellerstein, J. The Design of an Acquisitional Query Processor for Sensor Networks. *SIGMOD*, 2003.

[13] Madden, S., Franklin, M., Hellerstein, J., Hong, W. TAG: a Tiny AGgregation Service for Ad-Hoc Sensor Networks. *OSDI*, 2002.

[14] Madden, S., Szewczyk, R., Franklin, M., Culler, D. Supporting Aggregate Queries Over Ad-Hoc Wireless Sensor Networks. *IEEE WMCSA*, 2002.

[15] Manjhi, A., Nath, S., Gibbons, B. Tributaries and Deltas: Efficient and Robust Aggregation in Sensor Network Streams. *SIGMOD*, 2005.

[16] Mo, L., He, Y., Liu, Y., Zhao, J., Tang, S., Li, X., Dai, G. Canopy Closure Estimates with GreenOrbs: Sustainable Sensing in the Forest. *ACM SenSys*, 2009.

[17] Nath, S., Gibbons, P., Seshan, S., Anderson, Z. Synopsis Diffusion for Robust Aggregation in Sensor Networks. *SenSys*, 2004.

[18] Shnayder, V., Hempstead, M., Chen, B., Allen, G., Welsh, M. Simulating the Power Consumption of LargeScale Sensor Network Applications. *ACM SenSys*, 2004.

[19] Silberstein, A., Braynard, R., Yang, J. Constraint Chaining: On Energy-Efficient Continuous Monitoring in Sensor Networks. *SIGMOD*, 2006.

[20] Silberstein, A., Munagala, K., Yang, J. Energy-Efficient Monitoring of Extreme Values in Sensor Networks. *SIGMOD*, 2006.

[21] Wu, Y., Li, X., Liu, Y., Lou, W. Energy-Efficient Wake-up Scheduling for Data Collection and Aggregation. *IEEE TPDS*, 21(2):275-287, 2009.

[22] Yang, X., Lim, H., Özsu, M., Tan, K. In-Network Execution of Monitoring Queries in Sensor Networks. *SIGMOD*, 2007.